EFFECT OF PROCESSING ON TOPOLOGY AND HYDROPHOBICITY OF POLYDIMETHYLSILOXANE

Ting En Kam tkam564
Chemical and Materials Engineering 2017
Supervisor: Alisyn Nedoma

1. Abstract

The overall objective of this study was to investigate the factors that affect the topology and hydrophobicity of UV oxidized polydimethylsiloxane (PDMS), which included: magnitude of prestrain, film thickness and film width.

The wavelengths of wrinkles on oxidized PDMS was found using Fourier analysis, which showed an inverse relationship between prestrain and no relationship between film thickness and width.

Unexpected topological features were found on the nearly every measurement on the oxidized PDMS, namely areas of low amplitude sinusoidal waves or a single abnormally large peak in a regular sinusoidal wave. The reality of these “irregularities” were scrutinized, but no evidence against its presence was found. The cause of these irregularities was further explored, but no adequate solutions were found.

2. Acknowledgement

I would like to thank my supervisor, Alisyn Nedoma for her guidance and support throughout my project.

I would also like to thank Shifaz Khan. I would have not made it through the year without his moral support and encouragements.

Table of Contents

3. Introduction

Polydimethylsiloxane (PDMS) one of the most widely used silicon-based organic polymer due to its properties – inert, non-toxic and non-flammable [1]. For the common person, this substance is shiny and slippery and is used in shampoos or contact lenses. However, there are a lot of other applications beyond day-today uses such as medical devices and elastomers.

More recently, there have been a surge of research into nano-scale manipulation of PDMS topology, such as micropatterning of PDMS using UV light [2], micromolding of PDMS into nanogenerators [3]. To further research into nano-scale manipulation of PDMS and its use in medical devices, factors that affects the topology and hydrophobicity of PDMS in prestretched UV ozone processing were studied.

4. Project Aims and Objectives

The overall objective of this experiment was to investigate what effects prestrain of PDMS prior to UV oxidation, thickness and width of the PDMS film and have on the topology of the UV oxidized (glassy) PDMS. Specifically, the project can be broken into the following sections:

- To investigate the reliability and repeatability of experimental procedure
- To investigate the effect of film thickness, film width and extent of prestretch during UV oxidation on the topology of glassy PDMS
- To investigate the relationship between the hydrophobicity of PDMS and the topology of glassy PDMS
- To find and investigate any complexity that arise during the experiment

5. Background and Literature Review

5.1. Winkled PDMS as a Bacterial Inhibitor

Bacterial adhesion to surfaces and its survivability can be affected by materials with nanofeatured topographies [4] and the material's hydrophobicity. Interactions between bacteria species and surfaces are complex and unique to each species [4]. To effectively target specific bacteria, precise control over a material's topology and hydrophobicity is required. PDMS used in this project is synthesized using Sylgard 184. Sylgard 184 Silicone Elastomer is a two-part elastomer, consisting of Sylgard 184 Silicone Elastomer Base (PDMS monomer) and Sylgard 184 Silicone Elastomer Curing Agent (cross-linker).

5.2. PDMS

5.2.1. Hydrophobicity

By definition, a hydrophobic surface has a wetting contact angle of ≥ 90°. As a material, unmodified PDMS has a wetting angle of roughly 100° with water [5], making it a hydrophobic material. The contact angle of an ideal smooth surface can be determined by the Young–Laplace equation as shown below.

$$\gamma_{SG} - \gamma_{SL} - \gamma_{LG}\cos(\theta_C) = 0$$

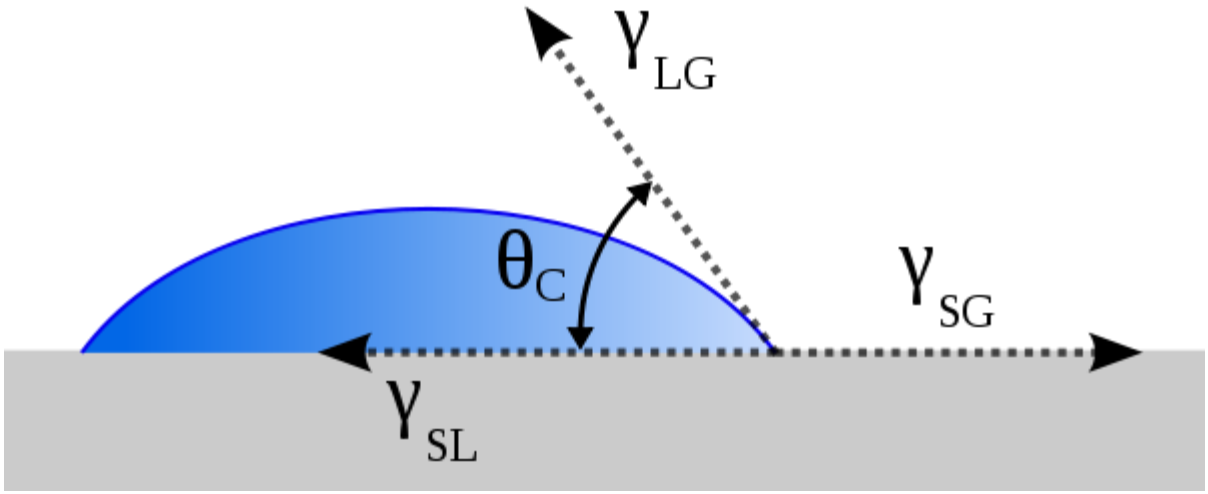

Figure 1: Schematic of a liquid drop showing the parameters in the Young equation. γ_{xy} refers to the interfacial energy of the x and y interface, where x and y are the solid (S), liquid (L) or gaseous (G) phase.

The Young – Laplace equation is based on the balancing of interfacial energy of the SL, SG, and LG interfaces.

Due to the roughness of our proposed surface, the Cassie-Baxter model is more appropriate. The wetting contact angle can be approximated using the following equation,

$$\cos\theta^* = f_1 \cos\theta_Y - f_2$$

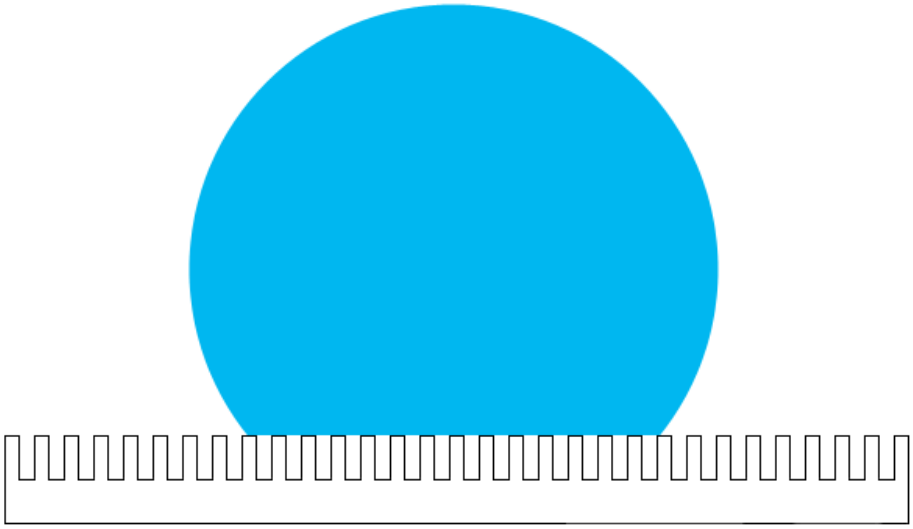

Figure 2: The Cassie-Baxter model.

Where f_1 and f_2 are the area fractions of solid and air under a drop on the solid surface, θ^* is the apparent contact angle and θ_Y is the equilibrium contact angle from Young – Laplace equation. From this model, it can be deduced that larger the area fraction of air, the greater the contact angle. As PDMS can be turned hydrophilic through UV oxidization [6], and the contact angle can be altered by the creation of microscale wrinkling on its surface, it can theoretically be made adequately hydrophobic or hydrophilic to counteract a given species of bacteria.

5.2.2. Modified Surface Topology: Wrinkled Glassy Layer

Nano-microscale wrinkling can be achieved through multiple approaches. In general, the procedures involve the creation of a bilayer of different modulus with internal stresses, which leads to mechanical buckling of the surface layer [7]. This experiment specifically utilizes the "plasma oxidation" method. This involves the pre-stretching of PDMS to create internal stresses, followed by plasma oxidation and stress release. This process creates sinusoidal wrinkles with characteristic profile wavelength and amplitude. The topology is a function of strain and the thickness of the glassy layer [7].

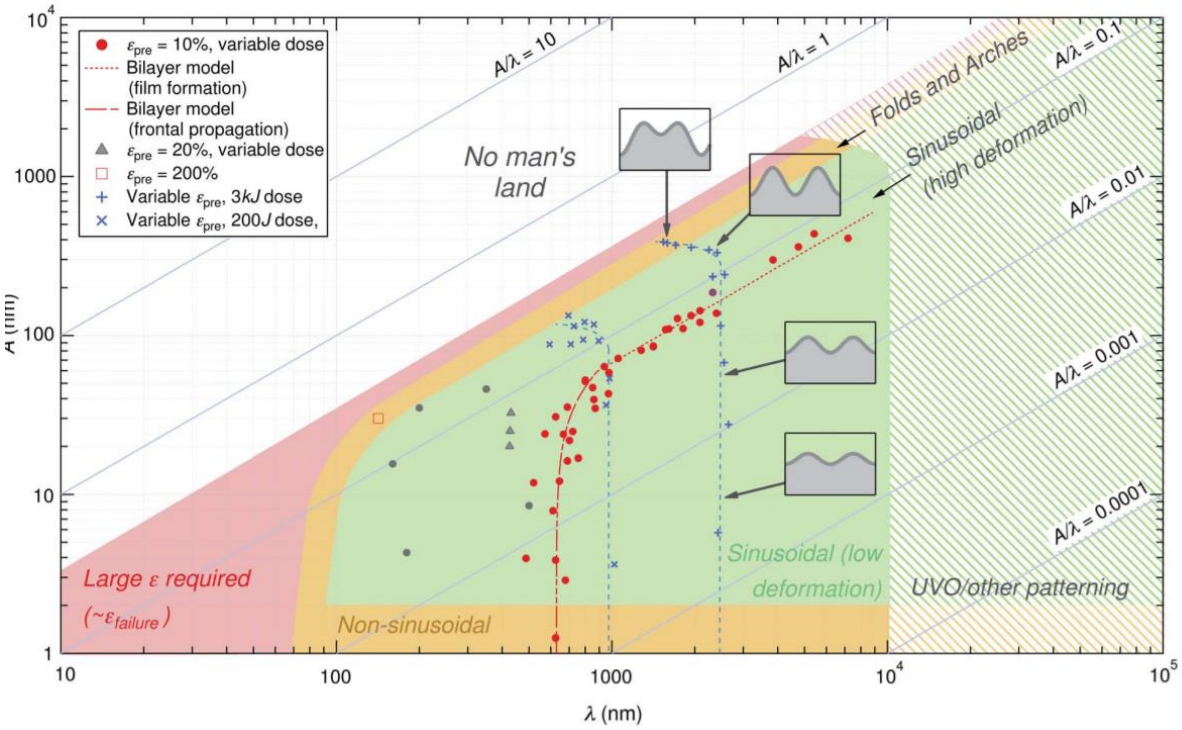

Figure 3:Wrinkling profile of PDMS reprinted from "Wavefront kinetics of plasma oxidation of polydimethylsiloxane" by Epstein AK et al.

The bombardment of PDMS with oxygen plasma strips it of its methyl group, $SiCH_3$, forming a thin glassy layer of silica, SiO_x or Si-OH [8].

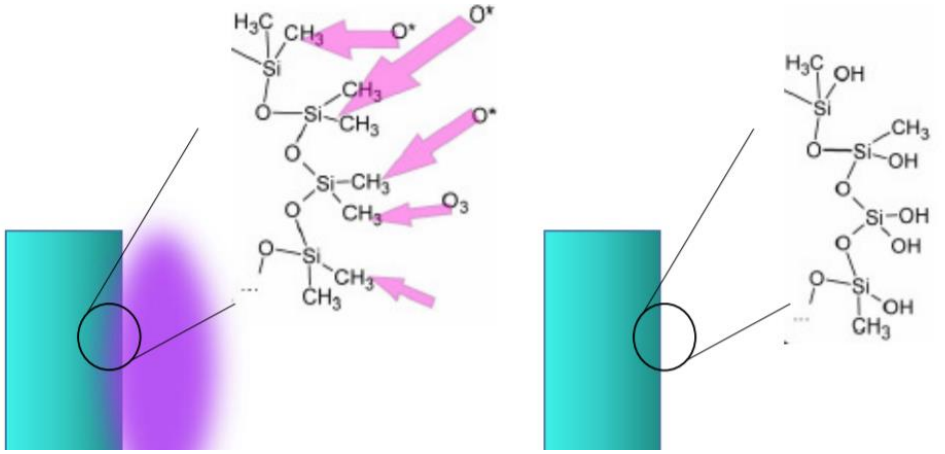

Figure 4: Figure 5: Schematic of oxygen treatment on PDMS, reprinted from Fabrication of Micro/Nano-Structured Wrinkles Through Surface Modification of Poly(dimethylsiloxane) by E. Daramola.

5.2.2.1. Fast Fourier Transformation

Fast Fourier transformation (FFT) is an algorithm that computes the discrete Fourier transform of a sequence. By utilizing Fourier analysis, a signal can be converted from its original domain to a representation in the frequency domain [9]. Due to the limitation of the Fourier analysis on excel, the series data must be 2^n in size, where n is an integer, and smaller or equal to 4096 in size [10].

5.3. Spin Coating

Spin coating is a procedure used to deposit uniform thin films onto flat substrates. The machine used for spin coating consists of a rotating vacuum stage to hold the substrate. The coating material (PDMS) is applied on the center of the substrate when it is not spinning. The substrate is then rotated at high speeds to create a thin film by centrifugal force. The thickness of the coating is a function of the revolution speed and viscosity of PDMS.

6. Materials and Methods

6.1. Methods

6.1.1. Polydimethylsiloxane Preparation

Objective: To ensure the polydimethylsiloxane (PDMS) samples created are of the same composition, and contain minimal air bubbles and impurities.

The PDMS produced is composed of two chemicals: PDMS monomer and cross-linker in a 9:1 weight ratio. 5g of the mixture is prepared every time a new batch is required. The following procedure was carried out to create the mixture.

PDMS prepolymer was drawn from the container using a disposable syringe from its container into a new plastic container. Cross-linker was drawn from its container using a different disposable syringe and added to the aforementioned plastic container. The mixture was mixed thoroughly (2 minutes) by hand using a metal stick to ensure homogeneity.

After mixing, the mixture was placed in a vacuum chamber for 20 minutes to remove any bubbles introduced during mixing. This step is to prevent localized stress concentration when the samples are stretched, which can lead to regions unusually low wrinkle wavelengths.

At 45 minutes from start of mixing, 6mL of the mixture were then spin coated onto a clean glass slide at various spin coating speeds (150 to 500) to vary its thickness, then left in a vacuum for an hour at 80℃ to cure. The timing of spin coating was regulated to reduce the variation in thickness caused by the increased viscosity from the slow curing of the mixture at ambient temperature.

6.1.1.1. UV Ozone Processing

Objective: To allow oxidation of PDMS surface in varying degree of strain and create samples of different wrinkle profiles.

2cm × 4cm samples of PDMS were removed from the aforementioned glass slide using a razor and attached on the stretching stage (Figure 5). The PDMS samples were fixed in place by the stage clamps. The samples were placed as close to parallel with the stage as possible to minimize any non-axial strain; the sample was tightly clamped to prevent slipping during the stretching.

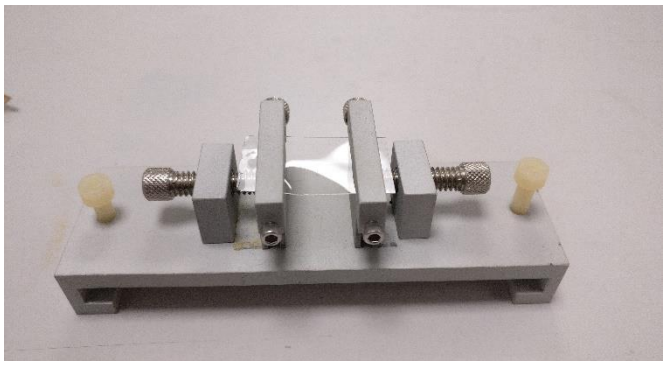

Figure 5: Stretching stage. Sample is currently not aligned parallel to the stage, which can lead to uneven strain

After stretching the sample, the sample and stage were exposed to oxygen plasma in the Novascan UV Ozone System (Figure 6) at 25℃ for 20 mins. The wattage of the machine is not changed as it is beyond the scope of this experiment. After the exposure, the sample is placed on a glass slide for later analysis.

With the exception of being unstretched, control glassy PDMS samples were created with the same procedure.

Figure 6: UV ozone system and ozone elimination system.

6.1.1.2. Profilometer

Objectives: This characterization technique was used to obtain and study changes in topology of PDMS samples after exposure to UV ozone at different strain.

Samples were either cured on glass slides or placed onto glass slides before setting it on the profilometer's stage. Initially measurements were taken on various points (Figure 12) of the sample to detect any variation of wrinkling profile on a single sample. Measurements were only taken from the center point of later samples.

The sampling resolution was set at a minimum of 4000 points per 1mm lateral. The stylus force used was 2mg.

To evaluate the machine's sensitivity to noise and the effectiveness of its dampening board (Figure 7), interference was deliberately introduced to the system by switching on a nearby pump during measurements. The produced 1D profile was compared to a repeated measurement of the same point.

Further tests were done to confirm the absence of any background noise in the system. This was done by repeatedly measuring a single section of a control PDMS sample at various sampling duration.

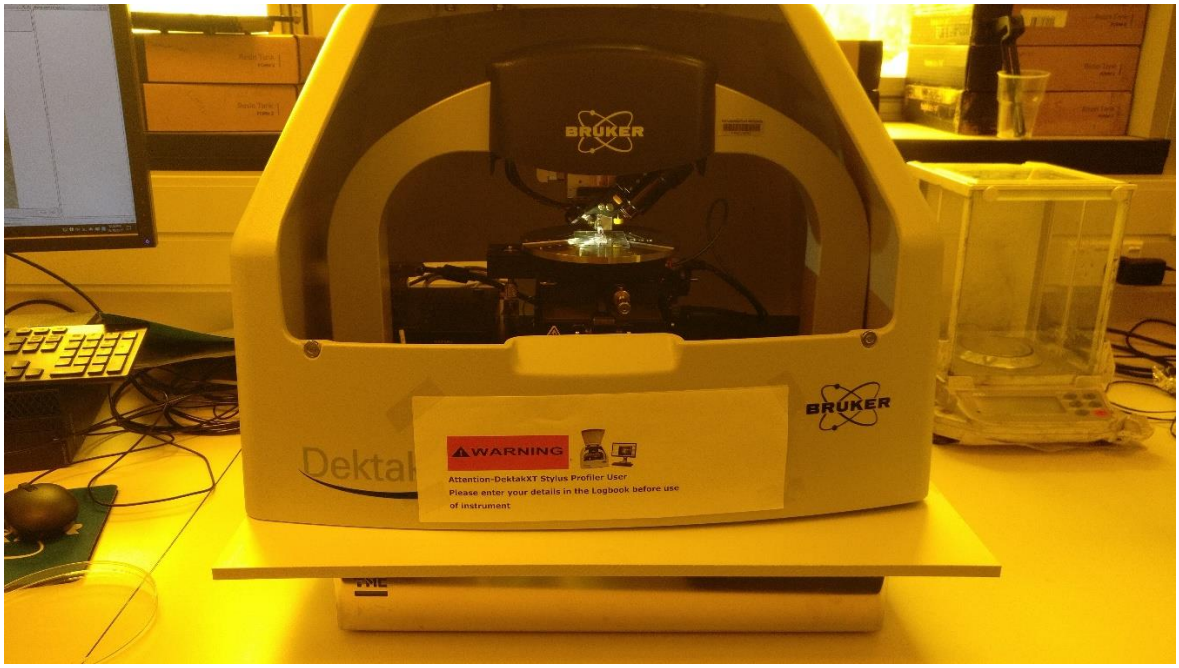

Figure 7: Profilometer on a dampening board.

6.1.2. Sessile Drop

Objective: This characterization technique was used to obtain and study changes in contact angle of samples after exposure to UV ozone at different strain.

Water droplets were deposited by a syringe which was positioned above the sample surface, and a camera captured the image from the side view. The image was processed using a software to determine its contact angle. Each data point given is based on 5 contact angle measurements at roughly the same point due to the small sample surface area.

6.1.3. Texture Analyzer

Objective: This characterization technique was used to obtain and study changes in the modulus of the samples after exposure to UV ozone at different strain.

Samples were secured onto the stretching rack and placed onto the Texture Probe CT table for analysis. A TA-PFS-C probe (Figure 8) was used for the test. Each data point given is based on 3 repeated tests.

Figure 8: TA-PFS-C probe as shown in the Texture Pro CT User Manual

The force applied by the probe onto the sample is converted engineering stress using the following equation:

$$\sigma = \frac{F_{parallel\ to\ sample}}{SA} = \frac{F_{probe}}{2\cos(\theta) \times (width \times height)_{sample}}$$

$$= \frac{F_{probe}}{2\left(\frac{l_i}{l_f}\right) \times w \times h}$$

$$\sigma = \frac{F_{probe}\sqrt{l_i^2 + x^2}}{2l_i wh}$$

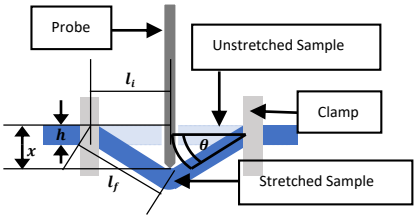

Figure 9: Diagrammatic representation of the texture analyser setup.

Whereas the probe distance, x is converted to strain using the following equation:

$$\varepsilon = \frac{l_f}{l_i} - 1 = \frac{\sqrt{l_i^2 + x^2}}{l_i} - 1$$

7. Results and Discussions

7.1. Topology

7.1.1. Noise and Control Analysis

To test the noise elimination ability of the profilometer, repeated tests were done on a single point of a control sample (cured PDMS) sample while noise was introduced to the system by the activation of a nearby pump.

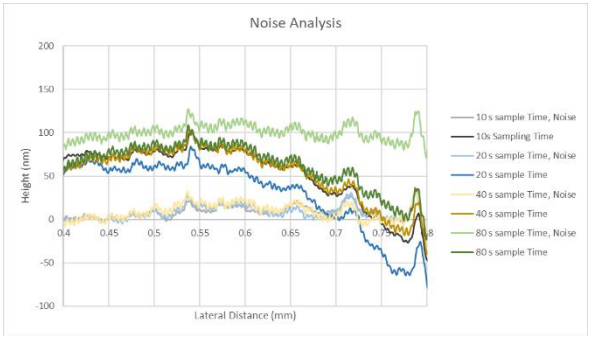

Figure 10: Repeated topological data of a single section of PDMS. A wavelength of roughly 5µm can be seen on all measurements.

The height value in Figure 10 is the vertical distance between sample height and a reference point. Despite repeated measurements of the same section, the reference point appears to shift by ±50nm. As such, only the profile of the wrinkles will be considered.

With the exception of samples taken with a sampling rate of 20s per 1mm, there is no visual evidence of difference between the wrinkling profiles of all tests with a wavelength of roughly 5µm. The amplitude of the wrinkles is roughly 5nm, which is greater than the 1nm found in literature [11]. It is possible that residual stress was developed during curing which lead to buckling in the control surface, but this is beyond the scope of this project.

To further scrutinize the data, Fast Fourier Transformation (FFT) was applied to the data. The following figure shows the FFT of the section.

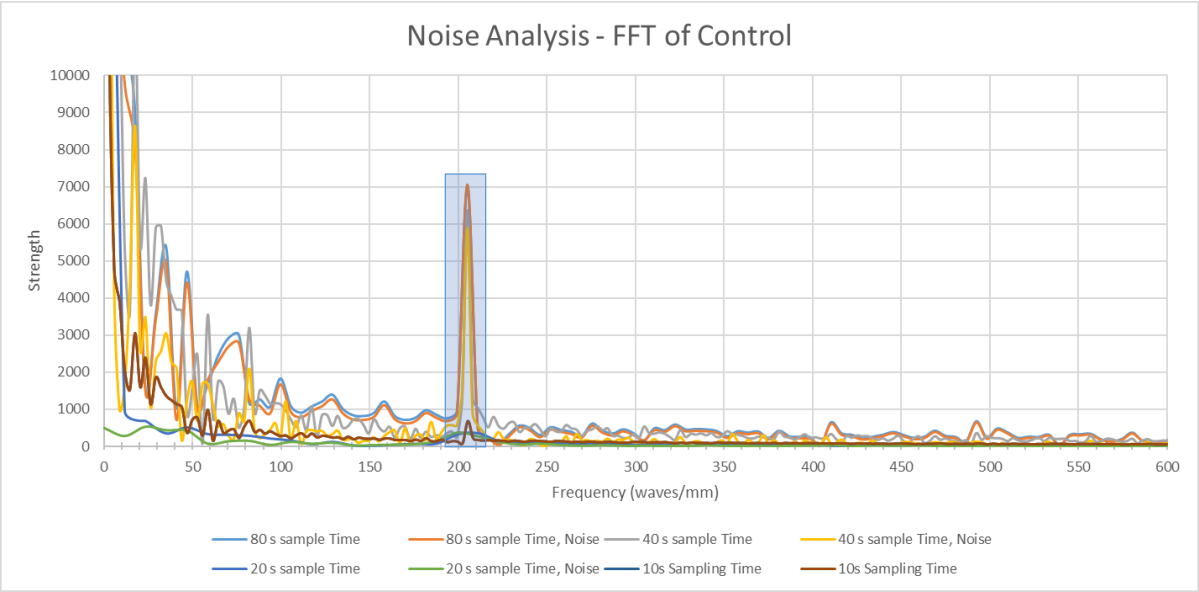

Figure 11: 8 sets of fast Fourier transformation of a section of topological data (Figure 10). Power increases exponentially as frequency approaches zero due to the curvature of the sample. All measurements included a relatively strong peak at around 205 waves/mm, which corresponds to the wavelength of 5µm seen in Figure 10.

7.1.2. Analysis of Spatial Variation

The following table shows the measured frequencies associated with the position on a 30% strain UV ozone processed PDMS. There are variations associated with the position of measurements. Generally, the further away the measuring position is from the center of the sample, the more likely it is to have no prominent wrinkles. The lack of prominent wrinkles is likely to be caused by the lack of strain applied in the area during exposure to UV ozone [12].

Improper securing of PDMS sample during UV ozone treatment is likely a contributing factor to variation, as it leads to non-uniform distribution of stress in the sample. Despite this, the range of wrinkle wavelengths is still relatively small (2.5 – 3.2µm). As such, all further analysis will be done with measurements taken from the center of the sample.

	Lateral Position			
Vertical Position	Major Frequencies (waves/mm)	1	2	3
	1	N/A	N/A	220-240 (Weak)
	2	N/A	N/A	N/A
	3	N/A	N/A	260-310
	4	330-390	320-390	370-430
	5	340-440	350-390	320-390
	6	310-340 390-410	N/A	370-400

Figure 13: Major frequencies associated with the given measurement on the positions shown on Figure 12. "N/A" denotes the lack of wrinkle profiles during measurements and prominent peaks found using FFT.

Figure 12: Positions of measurements. Measurements within the blue section are under strain during exposure to UV Ozone.

7.1.1. Relationship between Wrinkle Wavelength and Other Factors

With the exception of 50% strain, the wrinkle profile was inversely proportional to literature [13]. Wrinkling occurs due to the buckling of the glassy layer under the residual stress achieved through the plasm oxidation method. The increase in variance as strain increase is likely caused by improper restraining of samples to the stretching stage. Due to the flimsy clamps of the stretching stage, and the increase in internal stress as strain increase, the sample is more likely to dislodge from the stretching stage's clamps, resulting in higher variance at higher strain.

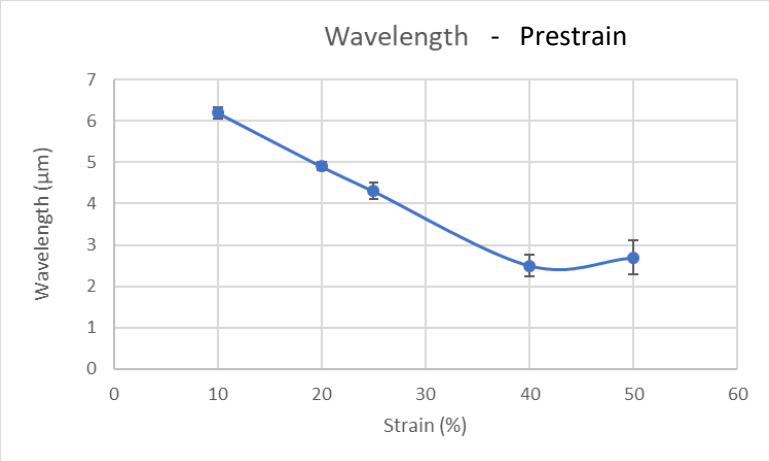

Figure 14: Relationship between prestrain and wrinkle wavelength. 3 samples were used for each data point.

There was no significant observable relationship between sample thickness (0.4mm to 0.6mm), sample width (10mm and 20mm) and the resultant wrinkle wavelength (4.2µm±2 at 25% strain). This consistent with literature – the wrinkling profile is a function of strain, thickness of glassy layer (affected by plasma oxidation time, which was unchanged) and the moduli of the bilayer.

7.1.1. Unusual Features

Most samples measured contained long sections of sinusoidal waves interspersed with regions of low amplitude sinusoidal waves or a single high amplitude peak similar to the figures below. These features appear to be irregular, and was not found in literature. Regions of low amplitude sinusoidal waves may be caused by cracks in the sample, resulting in sections of low internal stress and therefore low amplitude waves, however no sample was in the "cracking region" according to literature (Figure 3); It is possible that high amplitude spikes are caused by localized stress concentration that arise from the inclusion of small air bubbles (Figure 15). However, it is beyond the scope and capability of this experiment to locate the position of the small air bubbles and align the profilometer probe to the air bubble.

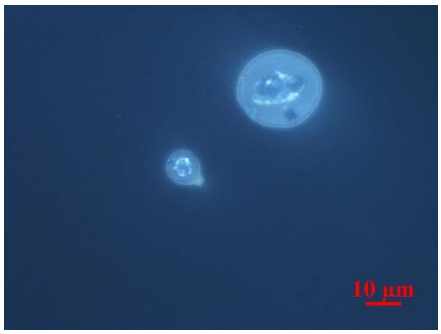

Figure 15: Air bubble inclusion in PDMS Samples

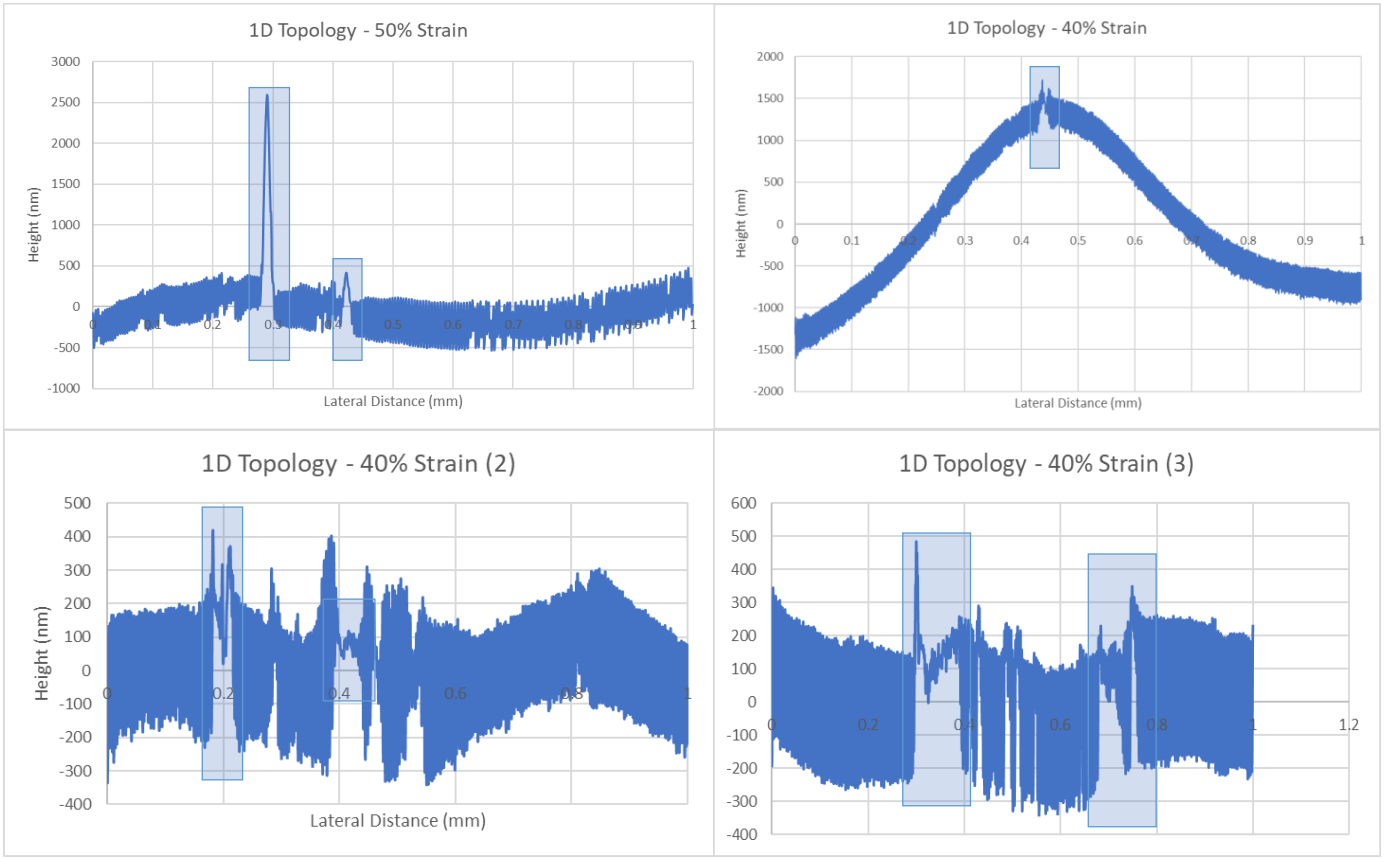

Figure 16: Example of measurements with unusual features. The unusual features are contained in blue containers

7.2. Hydrophobicity

As seen from the table below, glassy PDMS is hydrophilic whereas PDMS is hydrophobic. After the treatment, a decrease in wavelength leads to a decrease in contact angle. Literature supports this [14] where hydrophobic (contact angle < 90°) materials increases its hydrophobicity with decreasing wavelength and hydrophilic materials increases its hydrophilic with decreasing wavelength.

UV Ozone Processed	Stretched Batch	Wavelength (µm)	Contact Angle
		2.6	74.7
		4.3	83.1
	Unstretched Batch	-	63.7
Control PDMS		-	90.5

Figure 17: Relationship between contact angle and various factors.

7.3. Modulus

The curve produced from texture analyzer was transformed into a stress-strain curve (Figure 18) using the equation derived in 6.1.3 Texture Analyzer.

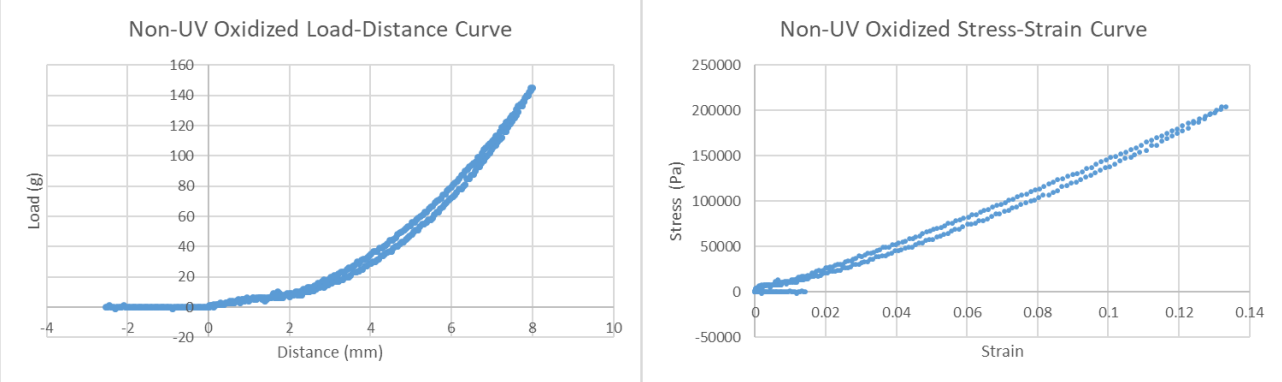

Figure 18: Example conversion from load-distance to stress-strain curve.

UV Oxidized		Non-UV Oxidized	
Sample	Young's Modulus (kPa)	Sample	Young's Modulus (kPa)
1	1324.731	1	1574.288
2	1447.5	2	1532.026
Average	1386.115	Average	1553.157

Figure 19: Young's Modulus of PDMS and Glassy PDMS-PDMS bilayer as calculated using the equation derived from 6.1.3 Texture Analyzer and gradient from the stress-strain curve produced.

The obtained PDMS modulus is similar to literature's 1.32MPa±0.7 [15]. As such, the measurement technique and accuracy is assumed to be reasonably accurate. It was found that UV Oxidized PDMS has a lower modulus than non-UV Oxidized PDMS. This is supported by the buckling of the glassy layer, as the glassy layer will not buckle if it was stiffer than PDMS.

8. Conclusion

- Low amplitude (5nm) wrinkles exist in control groups. Further analysis should be done to determine causes and mechanism involved.
- There is human and equipment caused variation in wrinkle wavelength. More reliable tools should be used for future experiments.
- An increase in prestrain during UV oxidation decreases wrinkle wavelength
- UV oxidation of PDMS converts the material from a hydrophobic material to a hydrophilic material
- Decrease in wrinkle wavelength after UV oxidation increases hydrophobicity of the glassy PDMS
- Further analysis of unusual features should be carried out, namely:
    - Factors that cause extreme peaks in prestrained UV oxidized PDMS
    - Factors that cause sparse regions of low amplitude sinusoidal waves in prestrained UV oxidized PDMS

9. References

[1] Dow Corning, "Sylgard® 184 Silicone Elastomer," 08 September 2017. [Online]. Available: http://www.dowcorning.com/DataFiles/090276fe80190b08.pdf. [Accessed November 2017].

[2] C.-Y. Xue, W. Zhang, K.-L. Yang and W. H. S. Choo, "Simplest Method for Creating Micropatterned Nanostructures on PDMS with UV Light," *Langmuir,* vol. 27, no. 22, pp. 13410-13414, 2011.

[3] J. Gong, G. Xu and X. Tao, "Breath Figure Micromolding Approach for Regulating the Microstructures of Polymeric Films for Triboelectric Nanogenerators," *Applied Materials & Interfaces,* vol. 9, no. 5, pp. 4988-4997, 2017.

[4] L. C. d. M. Dantas, J. P. d. Silva-Neto, T. S. Dantas, F. D. d. Neves and A. S. d. Mota, "Bacterial Adhesion and Surface Roughness for Different Clinical Techniques for Acrylic Polymethyl Methacrylate," *International Journal of Dentistry,* 2016.

[5] S. A. Y. P. D. A, "Superhydrophobic Surfaces Created by Elastic Instability of PDMS," *Applied Science (Switzerland),* vol. 6, p. 152, 2016.

[6] D. Bodas and C. Khan-Malek, "Formation of more stable hydrophilic surfaces of PDMS by plasma and chemical treatments," *Microelectronic Engineering,* vol. 83, no. 4-9, pp. 1277-1279, 2006.

[7] E. AK, H. D, K. P and A. J., "Wavefront kinetics of plasma oxidation of polydimethylsiloxane: limits for sub-mm wrinkling," *Soft Matter,* pp. 1155-1166, 2014.

[8] E. Daramola, "Fabrication of Micro/NanoStructured Wrinkles Through Surface Modification of Poly(dimethylsiloxane)," *Florida State University Thesis and Dissertation,* 2015.

[9] X.-S. Yang, Engineering Mathematics with Examples and Applications, Academic Press, 2017, pp. 173-185.

[10] P. T. Debevec, "The Excel FFT Function v1.2," 15 July 2018. [Online]. Available: http://physics.oregonstate.edu/~grahamat/COURSES/ph421/lec/ExcelFFT.pdf. [Accessed November 2017].

[11] E. Sarantopoulou, Z. Kollia, M. Kitsara and I. Raptis, "Entropic Nanothermodynamic potential from molecular trapping within photon induced nano-voids in photon processed PDMS layers," *Soft Matter,* vol. 8, p. 5561, 2012.

[12] D. Breid and A. J. Crosby, "Effect of stress state on wrinkle morphology," *Soft Matter,* no. 9, 2011.

[13] Y. Xuan, X. Guo, Y. Cui, C. Yuan, H. Ge, B. Cui and Y. Chen, "Crack-free controlled wrinkling of a bilayer film with a gradient interface," *Soft Matter,* no. 37, pp. 9603-9609, 2012.

[14] A. Sabbah, A. Youssef and P. Damman, "Superhydrophobic Surfaces Created by Elastic Instability of PDMS," *Applied Science,* 2016.

[15] I. D. Johnston, "Mechanical characterization of bulk Sylgard 184 for microfluidics and microengineering," *Journal of Micromechanics and Microengineering,* vol. 24, no. 3, 2014.

[16] A. Mata, A. J. Fleischman and S. Roy, "Characterization of Polydimethylsiloxane (PDMS) Properties for Biomedical Micro/Nanosystems," *Biomedical Microdevices,* vol. 7, no. 4, pp. 281-293, 2005.

[17] L. Liu, B. Ercan, L. Sun, K. S. Ziemer and T. J. Webster, "Understanding the Role of Polymer Surface Nanoscale Topography on Inhibiting Bacteria Adhesion and Growth," *ACS Biomater,* vol. 2, no. 1, pp. 122-130, 2016.

10. Appendix

10.1. Safety and Laboratory Use

HAZOP

Potential Hazards	Consequences	Preventative Action
Electrical equipment and wiring present	Injury/sprain from tripping over wires, electric shock (minor/major depending on situation)	Caution and care Ensure that cords are zip-corded neatly
Finger/hand getting under the hardness tester probe while in operation	Hand injury (minor/major depending on situation)	Make sure to keep hands away from the texture analyser when in operation.
Clothing or hair caught in the test	Injury, clothing damage	Keep clothing away from tester when in operation (loose sleeves, etc)
Spillage of prepolymer	Causes a slip hazard, contaminates surrounding area unless cleaned thoroughly	Caution and care Ensure that mixing is done at a reasonable speed and containers are well placed
Using an oven	Burns	Use appropriate safety gear when placing samples inside a hot oven and when taking them out (gloves)
Using a UV box	Skin burns, eye inflammation. Health effects vary with the duration of exposure as well as the intensity and wavelength of the energy.	Wear appropriate PPE (lab coats, gloves, safety glasses, face shields). Be aware of gaps in protection at the wrist or neckline.